Chemical and Biological Remediation of Lindane Residue in Aqueous Media

Ahmed Massoud[1]; Aly Derbalah[1]; Ibrahim El-Mehasseb[2]

and Moustafa Saad Allah[1]

[1]Pesticides Chemistry and Toxicology Department, Faculty of Agriculture, Kafr-El-Sheikh University, 33516 Egypt. [2]Chemistry Department, Faculty of Science, Kafr-El-Sheikh University, 33516 Egypt

Abstract

This study was carried out to evaluate the efficiencies of chemical remediation by advanced oxidation processes [TiO_2(nano /H_2O_2/UV, ZnO(nano)/H_2O_2/UV, Fe^{2+}/H_2O_2/UV, Fe^{3+}/H_2O_2/UV, TiO_2/H_2O_2/UV, ZnO/H_2O_2/UV, H_2O_2/UV and UV] and bioremediation by *Xanthomonas campestris pv. Translucens* and *Aspergillus fumigatus* for removal of lindane residue for aqueous media. To confirm the total detoxification of lindane residue in treated water, toxicity test was carried out using the most effect chemical and biological treatments with respect to histological changes in kidney and liver of treated rats relative to control. Nano zinc oxide and titanium dioxide combined with hydrogen peroxide under UV light was the most effective treatments for lindane removal in water. Bioremediation of lindane by *Xanthomonas campestris pv. Translucens* and *Aspergillus fumigatus* removed more than 94 and 84% of lindane initial concentration after 32 days of treatment respectively. There is no remaining toxicity in lindane contaminated-water after remediation with the most effective chemical and biological treatments (ZnO (nano)/H_2O_2/UVand *Xanthomonas campestris pv. Translucens*) on treated rats relative to control. Advanced oxidation processes especially with nanomaterials and

bioremediation can be regarded as safe and effective remediation technologies for lindane in water.

Keywords: water, pollution, lindane, remediation, toxicity

1.Introduction

For the first time in the history of the world, every human being is now subjected to contact with dangerous chemicals, from the moment of conception until death. The synthetic pesticides have been so thoroughly distributed throughout the animate and inanimate world that they occur virtually every where. Residues of these chemicals have entered and lodged in the bodies of fish, birds and they have been found in water and in man himself **(Carson 1962).**

After more than fifty years from Rachel Carson's cry the environmental problems are still in focus to day, through the development of the agrochemical industry, it has dramatically increased due to the wide spread intensive agriculture. Consequently, human health is threatened by concentration of pesticide, heavy metals, hydrocarbons, chlorinated hydrocarbon, etc….., present in continental and marine natural water as a results of industrial effluents **(Beziuk *et al.*, 1996; Oller *et al.*, 2006)**.

Water pre- requisite for life and key reasons of humanity, is abundant on earth. However, 97% is salt water. The remaining 2.5% that is the- fresh water, 70% is frozen in the polar ice caps. Only less than 1% of the world's fresh water resources are readily available for human use **(WHO 2002),** 2.2 million people in developing countries, most of them children, die every year from diseases as associated with a lack of safe drinking water, in adequate sanitation and poor hygiene **(WHO 2000; UNICEF 2000)**.

Egypt, today is facing and suffering from tow huge problems. The first one is the Renaissance Dam in Ethiopia, it can cause a shortage in water supply and reduction Egypt's share of the Nile water by 14.5 billion cubic meters, which can irrigate 3 million Feddan and the second problem is the environmental pollution in general, and particularly agrochemical pollutants in surface water through the intensive used of pesticides and fertilizers.

On the other hand, the pollution of surface water and wastewater has increased sharply and it constitutes a major problem due to an extensive use of these substances **(Evgenidou *et al.*, 2007).** The monitoring of pesticides in surface water showed the presence of organochlorines, organophosphorus and carbamates insecticides in water resources in Kafr El-sheikh Governorate **(Hamed 1997; Abd El-Razik, 2007a; Massoud *et al.*, 2011; Ismail *et al.*, 2015)**.

Removal of heavily used insecticides and their photoproducts from aquatic environment have become a very important task for human being. Thus, advanced oxidation processes (AOPs) methods are in demand for effective treatment of pesticides-polluted water to achieve complete mineralization of target pesticides and to avoid the formation of toxic end products (**Derbalah *et al.*, 2011; El-Fakharany *et al.*, 2011; Massoud *et al.*, 2011)**.

Nanotechnology is an emerging technology, which can lead to a new revolution in every field of science (Rico et al., 2011). Nanostructured semiconductors as zinc oxide (ZnO) and titanium dioxide (TiO2) are a potential

candidate for the mineralization of toxic organic compounds, hazardous in organic constituent (Curri et al. 2003) .

Pesticide contamination of surface water and ground water from agricultural use has been a concern for a long time. Attention is usually focused on contamination by organochlorine pesticides

Organochlorine pesticides (OCPs) due to their toxicity and persistence in environment. Therefore, organochlorine monitoring and measurements in fresh water need to be further developed by providing analytical tools to carry out advanced monitoring strategies in the environmental analysis.

Advanced oxidation processes (AOPs), which are constituted by the combination of several oxidants, are characterized by the generation of very reactive and oxidizing free radicals in aqueous solution such as hydroxyl radicals, which posses a great destruction power (**Benitez et al. 2002; Evgenidou et al. 2005;**). Bioremediation of hazardous wastes is a relatively new technology that has undergone more intense investigation as of recent decades. This process is focused on destroying or immobilizing toxic waste materials **(Shannon and Unterman, 1993)**. Bioremediation is an option that offers the possibility to destroy or render harmless various contaminants using natural biological activity. As such, it uses relatively low-cost, low-technology techniques, which generally have a high public acceptance and can often be carried out on site **(Vidali 2001)**.

However after remediation of pesticide residues in water, toxicity assessment is needed after remediation of pesticide residues in water to directly assess the potential hazard of both original pollutants and its metabolites (**Derbalah, 2009**).

In this study the efficiency of advanced oxidation processes materials with synthesis Zinc Oxide and Titanium Dioxide nanoparticles, in addition to Photo Fenton reaction , and moreover the bioremediation with *Xanthomonas campestris pv. Translucens* and *Aspergillus fumigatus* were evaluated to achieve the total degradation of lindane. The enzymes activity and histological changes in liver and kidney of rats was measured to confirm the complete detoxification of lindane-contaminated water.

2.Materials and Methods

2.1. Chemicals

Lindane with purity of 99.5% was obtained from Kafr El-zayat Company for Chemicals and Pesticides, Egypt. Zinc oxide (99.99%) and titanium dioxide (99.9%) nanoparticles were synthesized and characterized in the Nanotechnology Centre in Faculty of Science, Kafr El-shiekh University, Egypt. The shape and size of zinc and titanium oxides nanoparticles were shown in the part of results and discussion.

2.2. Chemicals for synthesis of nanoparticles (NPs)

Zinc acetate dihydrate $Zn(CH_3COO)_2.2H_2O$ with 99.5 % purity was obtained from Loba Chemie, Mumbai, India. Triethyl amine (TEA) $(C_2H_5)_3N$ with 99 % purity was obtained from Alpha Chemika Company, Mumbai, India. Titanium tetrachloride ($TiCl_4$) with 98% purity was obtained from BHD Limited Pode Company, England. Ethyl alcohol (ethanol) C_2H_5OH with 95 % purity was obtained from Piochem for Laboratory Chemicals Company, Cairo,

Egypt. Zinc nitrate hexahydrate $Zn(NO_3)_2.6H_2O$ with 99% purity was obtained from Winlab Company for Laboratory Fine Chemicals, India. Hexa methylene tetra amine ($C_6H_{12}N_4$) with 99 % purity was obtained from Alpha Chemika Company, Mumbai, India.

2.2.1.Synthesis of nanomaterials

ZnO nanoparticles (NPs)

Zinc acetate dihydrate ($ZnAc_2.2H_2O$) and capping agent (triethylamine, TEA) were mixed at a molar ratio of 5:3 in ethanol according to (**El-Kemary *et al.*, 2010)**.

TiO_2 nanoparticles (NPs)

Nanostructured TiO_2 catalysts have been prepared by hydrolysis of titanium isopropoxide or titanium tetrachloride according to **(Addamo *et al.*, 2004)**.

2.3.Photochemical remediation

The scope of the experiments included the following treatments: Nano titanium dioxide combined with hydrogen peroxide(TiO_2 (nano)/H_2O_2/UV), nano photo zinc oxide combined with hydrogen peroxide (ZnO (nano)/H_2O_2/UV), photo Fenton reagent (Fe^{2+}/H_2O_2/UV), photo titanium dioxide combined with hydrogen peroxide (TiO_2 /H_2O_2/UV) and photo zinc oxide combined with hydrogen peroxide (ZnO/H_2O_2/UV).

For photo Fenon and Fenton like reaction UV Lamp as employed for the irradiation of lindane in aquatic solution. Ferric chloride and ferrous sulphate were used as source of iron catalyst**.** The solution was prepared by addition of desired amount of lindane (5 mg L^{-1}) distilled water and carefully agitated. Then, freshly prepared ferric

chloride or ferrous sulphate at concentration level of 50 mg L^{-1} as Fe^{3+} was added followed by the addition of H_2O_2 at concentration level of 20mg/L. After that the solution was completed with water up to 1000 mL. The initial pH of the solution was adjusted to be 2.8 by using hydrochloric acid 1 Molar for all experiments **[Derbalah et al. 2004].** The solution was transferred from the standard flask to quartz glass cell (1000 mL) and exposed to the irradiation of the UV lamp under constant temperature of 25°C with steering (the distance between the lamp and lindane solution 15 cm).The solutions from the irradiated samples were removed at regular intervals (0,10, 20, 40,60, 80, 160,320 and 360 min) for HPLC analysis.

For ZnO and TiO_2 catalysts (nano or normal size), lindane at concentration level of 5mg L^{-1} with appropriate amount of ZnO or TiO_2 (300 mg L^{-1}) was shacked carefully before illumination followed by the addition of H_2O_2 at concentration level of 20mg/L. Then the pH was adjusted to 7, the optimum pH for ZnO or TiO_2 catalysts**.** The suspension was kept for 30 min in the dark, prior illumination to achieve the maximum adsorption of the pesticide onto semiconductor surface. On the other hand, blank degradation experiments were carried out at dark. The solutions from the irradiated samples were removed at regular intervals (filtered by Millipore syringe filter of 0.45 μm) for HPLC analysis as mentioned before elsewhere. Each experiment was replicated three times for accurate data.

2.4.HPLC analysis

The irradiated samples were analyzed directly by HPLC system in the Central Laboratory of Pesticides, Agriculture Research Center, El-Dokey, Cairo, Egypt.

In the case of lindane a mixture of methanol and distilled water (85: 15) was used as mobile phase under the isocratic elution mode. The flow rate of mobile phase was maintained at 0.8 ml min^{-1} and the column type used was C8 Zorbax (250 mm×4.6 mm×5µm). The used detector was UV and the wavelength was 254 nm at retention time was 4.884 min.

2.5.Bioremediation technique

The bioremediation test was carried out at pesticides laboratory, Dep. of Pesticides chemistry and Toxicity, Fac. of Agric. Kafrelsheikh Univ. The selected microbial isolates (A1) *Aspergillius fumigatus and* (A2) *Xanthomonas campestris pv. Translucens* were cultured onto MSL spiked with the tested insecticides (lindane), separately for 7 days and then the growing colonies were washed with three ml sterilized MSL liquid medium. The cell suspension of 10^8cfu/ml (cfu:colony forming unit) was used to inoculate 100 ml MSL liquid medium containing 5ppm of the tested insecticide.

The cultures were incubated at 30 ºC, pH (7) **(Massoud *et al*., 2007b; Derbalah and Belal, 2008)** and 150 rpm as optimum conditions for the growth of the tested microbial isolate for 32 days. Samples were collected at 0, 4, 8, 12, 16, 20, 24, 28, and 32 days for monitoring the parent compound degradation of the tested insecticides. Control flasks of equal volume of MSL liquid medium and the tested insecticides without the selected microbial isolates were run in parallel at all intervals to asses a biotic loss. The collected water samples of the tested insecticide were filtered using syringe filtered **(Massoud *et al*., 2008)** followed by HPLC analysis as mentioned before for each insecticide.

2.6.Toxicity experiment

To confirm the complete detoxification of polluted water with lindane and exposed to chemical remediation by advanced oxidation process in the presence of $ZnO/H_2O_2/UV$ toxicity test was conducted on rats. The same test was done in the presence of *Xanthomonas campestris pv. Translucens*; water, orally administrated to the tested rats. This test was carried out to measure the effect of the possible remaining lindane (parent or metabolites) in the water samples after remediation on rats with respect to histological changes in liver and kidney of treated rat's relative to control.

Adult rats (*Sprague Dawley*) with 100-120 gm of weight, obtained from Faculty of Veterinary Medicine, Kafr-El-Shiekh University were used. Rats were housed in polypropylene cages under standard conditions with free access to drinking water and food. The animals were randomly divided into five groups each comprising of three animals and the treated samples that possibly contain lindane were given to rats as oral administration. Control group rats were fed with normal diet and given oral dose containing no lindane. After 28 days, the rats were scarified under anesthesia and the kidney and liver organs were removed and prepared for histopathological examination according to the method described by **Bancroft and Stevens (1996)**. The histopathology test was carried out at Dep. of Histopathology, Fac. of Veterinary Medicine, Cairo Univ. Egypt.

3.Results and Discussion

3.1.Characterization of synthesized and commercial materials

Physical characterization of synthesized ZnO and TiO2 were carried out using UV-visible spectrometer, X-ray diffraction (XRD), Fourier transformed infrared spectroscopy (FTIR), thermos gravimetric analysis (TGA), transmission electron microscope (TEM), and scanning electron microscope (SEM) analysis, while physical characterization of synthesized ZnO (s) immobilized on fluorine doped tin oxide glass (FTO) (thin film) was investigated by XRD and SEM analysis. On the other hand, physical characterization of commercial ZnO and TiO2 were carried out using UV-visible spectrometer, X-ray diffraction (XRD), (FTIR),(TEM) and (SEM) analysis.

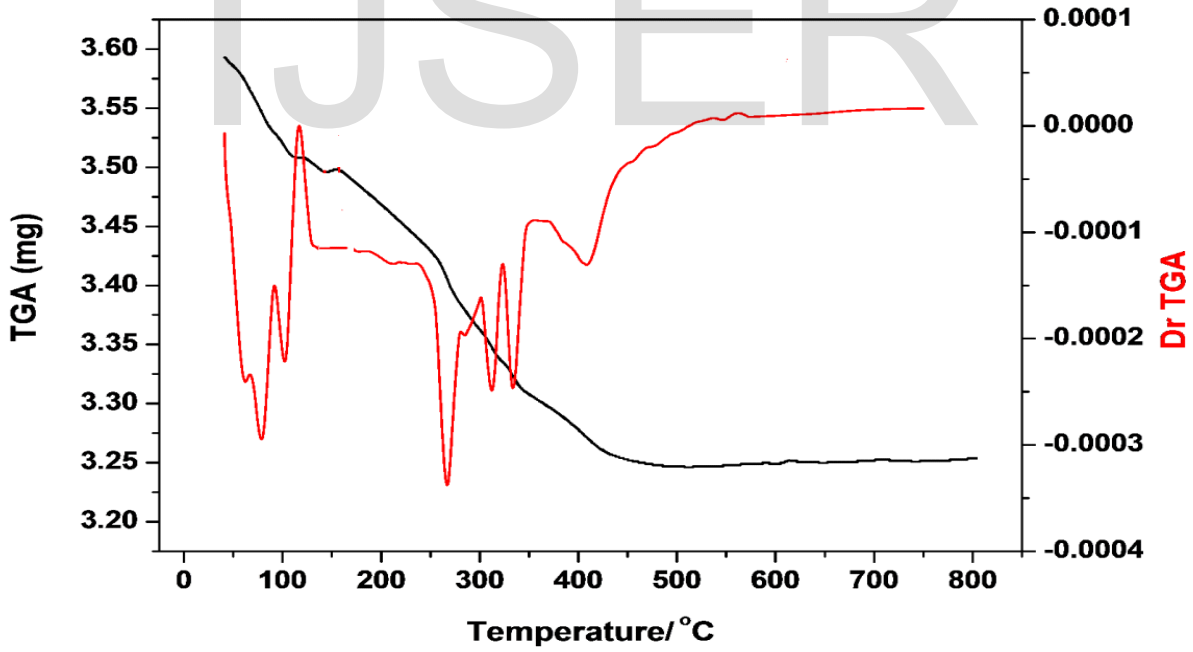

Fig. (1): TGA-DrTGA of the synthesized ZnO isolated at a heating rate of 10 ^{o}C/min under nitrogen atmosphere.

Fig.(1) show a plot of TGA-Dr TGA of ZnO (NPs). The synthesized sample was heated from room temperature to 800 C with heating rate of 10°C/ min. under nitrogen atmosphere. The most observed weight loss of ZnO(Nano) takes place before 450°C. Total weight loss was about 9.7% in three stages attributed to the loss of water, solvent and some acetate as byproducts of the reaction . The thermos gravimetric curve reflects a nearly flat till 800°C ; this is a good evidence for formation of a thermal stable ZnO (NPs). The same analysis was done with TiO2 (NPs).

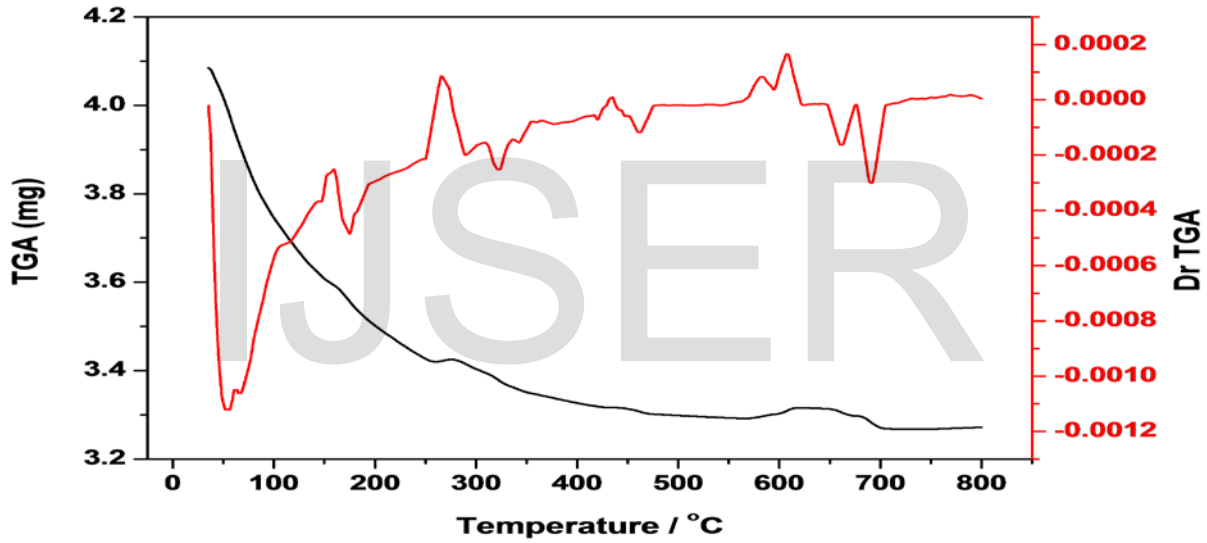

Fig.(2): TGA-DrTGA of the synthesized TiO_2 powders measured at a heating rate of 10 ^{o}C/min under nitrogen atmosphere.

The results are shown in Fig. (2) The synthesized TiO2 powder was measured for its thermal properties from room temperature to 800 C under nitrogen atmosphere at heating rate of 10 C/min. Evidently, the weight loss proceeded in stages with increasing temperature, while the most significant weight loss occurred before 500°C , this weight loss is due to the elimination of hydrated and coordinated of water

molecule as well as the decomposition products of the adsorbed trimethylamine. After 500°C, the thermogravimetric curve showed a nearly flat characteristic of weight loss except of the increment of the adsorbed gases at 500C-620°C which indicate that the pure TiO2 was formed at 500°C. Values of X-ray parameters of synthesized ZnO.

Table (1): Values of X-ray parameters of synthesized ZnO.

Peak No.	2θ	d (°A)	FWHM	Size (nm.)
1	31.4105	2.84570	0.4323	34.0
2	34.0696	2.62944	0.39710	36.5
3	35.9002	2.49944	0.4170	34.5
4	56.2741	1.63344	0.42430	37.04
5	62.5421	1.48395	0.44020	36.8
6	67.6417	1.38394	0.42060	39.7

Table (2): Values of X-ray parameters of commercial ZnO.

Peak No.	2θ	d (°A)	FWHM	Size (nm.)
1	31.4316	2.8438	0.23350	61.66
2	34.0889	2.62799	0.22600	64.14
3	35.9223	2.49796	0.23080	63.12
4	47.2246	1.92313	0.22390	67.55
5	56.2925	1.63295	0.22370	70.28
6	62.5689	1.48338	0.22200	73.05
7	67.6633	1.38355	0.22010	75.8

Table (3): Values of X-ray parameters of synthesized TiO_2.

Peak No.	2θ	d (°A)	FWHM	Size (nm.)
1	25.3240	3.51416	1.24800	11.39
2	30.8575	2.89543	0.36500	39.4
3	47.5700	1.90997	0.20660	73.3
4	48.2500	1.88462	0.56000	27.00
5	54.2920	1.68829	0.26400	59.00

Table (4): Values of X-ray parameters (antase).

No.	2θ	d (°A)	FWHM	Size (nm.)
1	25.0598	3.55060	0.21750	65.27
2	47.8348	1.90001	0.20390	74.35
3	37.5705	2.39207	0.21900	66.84
4	54.8692	1.67189	0.20970	74.46
5	62.4999	1.48485	0.21850	74.19
6	74.8786	1.26711	0.22060	79.12

3.1.1.Fourier transformed infrared spectroscopy (FTIR)

Figure (3 a and b) shows FTIR spectra of the synthesized ZnO (s) ,infrared studies were carried out in order to ascertain the purity and nature of the metal nanoparticles. The peaks observed in Fig. 3 at 3455 and 1083 cm^{-1} are may be due to O-H stretching and deformation, respectively assigned to the water adsorption on the metal surface. The peaks at 1634, and 537 cm^{-1} are corresponding to Zn-O stretching and deformation vibration , respectively. The metal –oxygen frequencies observed for the respective metal oxides are in agreement with (Markova-Deneva 2010) and (Parthasarathi and Thilagavathi .2011); they reported that, similar FTIR spectra

observed of ZnO nanoparticles . Figure 17b shows the observed peaks of commercial zinc oxide ,two peaks at 3441 and 1089 cm^{-1} could be revealed to O-H stretching and deformation ,respectively assigned to the adsorbed water on the metal surface. The peaks at 1631, and 537 cm^{-1} are corresponding to Zn-O stretching and deformation vibration, respectively.

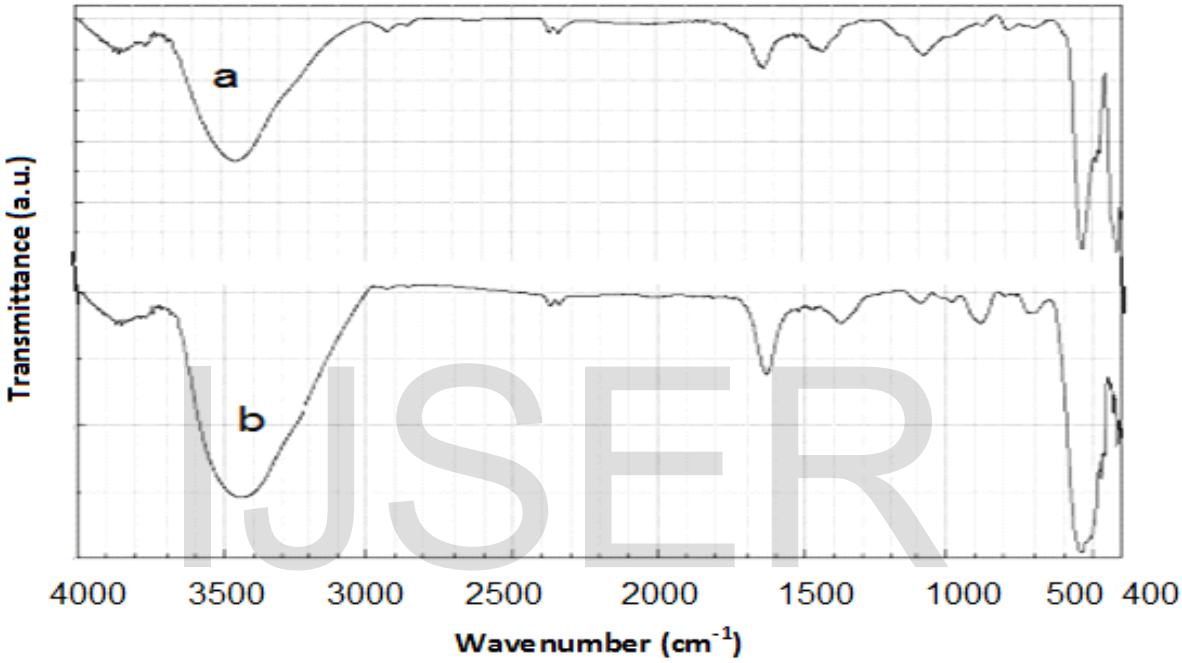

Fig. (3): FTIR spectroscopy of (a) synthesized and (b) commercial ZnO.

3.1.2.FTIR spectroscopy of synthesized and commercial titanium dioxide

Figure (4 a and b) shows the FTIR spectra of the synthesized and commercial TiO_2 in the range of 400-4000 cm^{-1} respectively. The Figure (4a) depicts that, the synthesized TiO_2(s) shows the peaks at 449 cm^{-1} is for O-Ti-O bonding **(Yu *et al.*, 2003)**. The band centered at 1622 cm^{-1} is a characteristic peak of δ-H_2O bending **(Karakitsou and Verykios, 1993)**. Figure (4 b) shows the commercial TiO_2, the peaks at 438 cm^{-1} is for O-Ti-O bonding. The band centered at 1632 cm^{-1} is a characteristic peak of δ-H_2O bending.

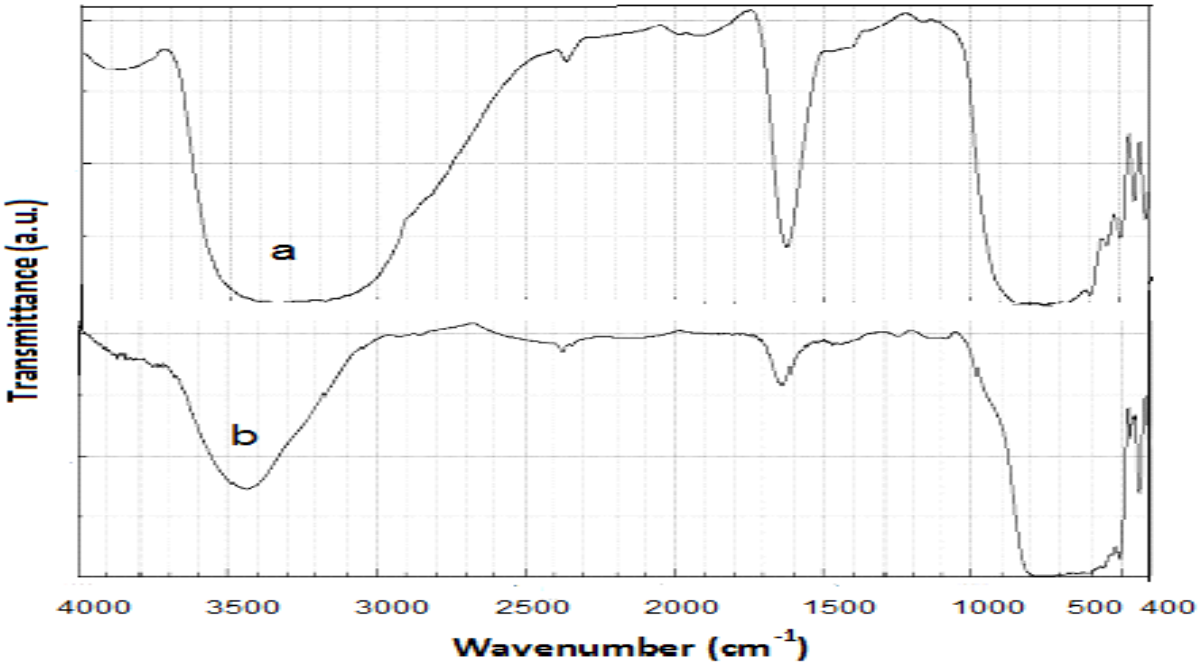

Fig. (4): FTIR spectroscopy of (a) the synthized and (b) commercial TiO_2.

3.1.3.UV-Visible spectroscopy analysis

UV-Visible Spectra of ZnO

The room temperature UV-Vis absorption spectra of an aqueous solution ZnO for synthesized and commercial were measured and are shown in Fig. (5 a and b). ZnO particles were dispersed in deionized water with a suitable concentration and then the solution was used to perform the UV-Vis measurement. The spectrum shows an absorption peak of the synthesized ZnO at wavelength of 368.5 nm, Fig. (5 a) and at 376.2 nm, Fig. (5b) of the commercial which can be assigned to the intrinsic band gap absorption of ZnO due to the electron transitions from the valence band to the conduction band (**Yu *et al.*, 2006**).

The band gap energy (E) was calculated as per the literature report using the following equation (**Hoffmann *et al.*, 1995**):

Band gap energy (E) =hc / λ

Where h is the Plank's constant (6.625×10^{-34} Js), c is the speed of light (3.0×10^{8} m/s) and (λ) is the wavelength.

According to this equation, the band gap of the synthesized ZnO(s) is 3.36 eV while the band gap of the commercial ZnO is 3.29 eV. The wide band gap energy of semiconductor nanoparticles is the more reactive in a photocatlytic degradation of the organic pollutants **(Dhal *et al.*, 2015)**.

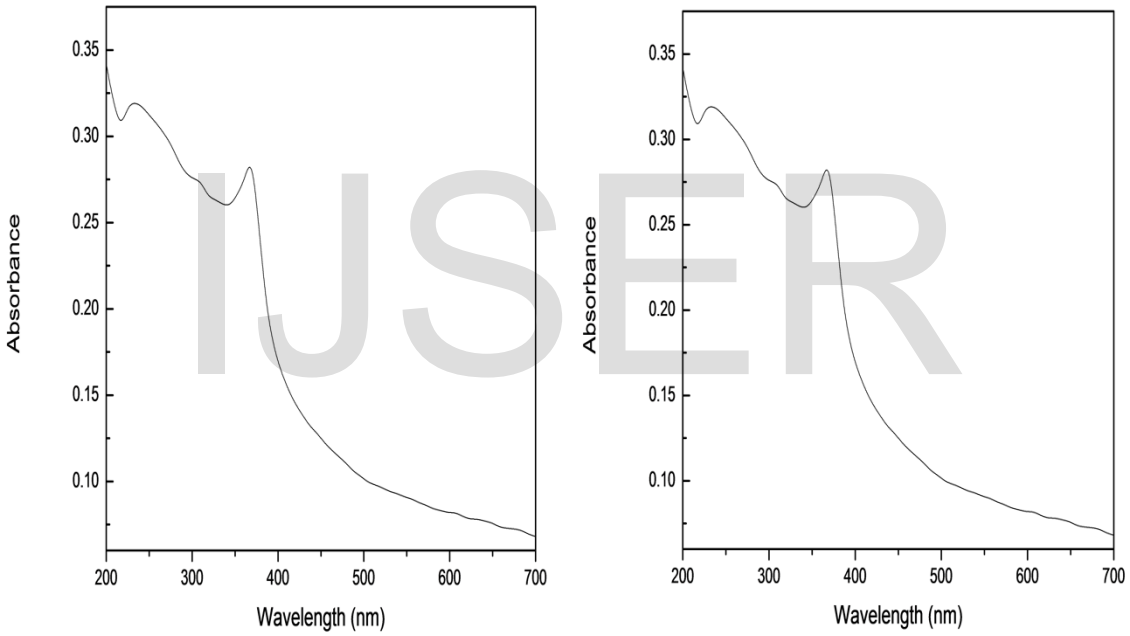

(a) (b)

Fig. (5): UV-Vis absorption spectra of an aqueous solutions of (a) the synthesized and (b) commercial ZnO.

3.1.4.UV-Visible Spectra of TiO_2

For the study of the optical properties of the synthesized and commercial TiO_2 nanoparticles, the band gap and the type of electronic transition were determined, which were calculated by means of the optical absorption spectrum (**Essick and Mather, 1993**). When a semiconductor absorbs photons of energy larger than the gap of the semiconductor, an electron is transferred from the valence band to the conduction band where there occurs an abrupt increase in the absorbency of the material to the wavelength corresponding to the band gap energy.

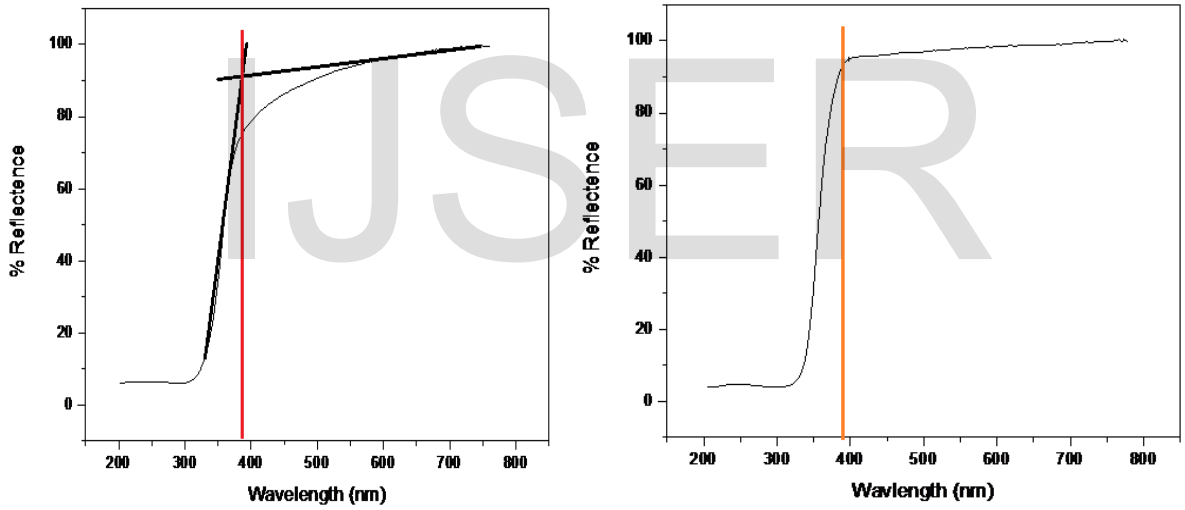

(a) (b)

Fig. (6): Diffuse reflectance UV-Vis spectra of synthesized TiO_2 (a) and commercial TiO_2 (b).

The band gaps are 3.19 and 3.16 eV for synthesized and commercial TiO_2 which are in agreement with their surface areas. The small particle size of the synthesized TiO_2 which has a high surface area and consequently it has high activity for organic pollutants degradation **(Curri *et al.*, 2003; Nurmi *et al.*, 2005; Dhal *et al.*, 2015**).

3.1.5.Scanning Electron Microscope (SEM)

Figures (7 and 8) show typical scanning electron images of synthesized, commercial and the thin film of semiconductor ZnO depositeted on FTO substrate glass. Results indicate that, the shape of the synthesized ZnO is spherically shape with diameter in the range of 30-49 nm (Figure 7). The commercial ZnO (Figure 8) appears as randomly oriented hexagonal prisms with diameter ranged from 34 to 119 nm and with length ranged from 169 to 399 nm.

Figures 9 and 10 are the SEM images of the synthesized and commercial TiO_2, respectively. The synthesized TiO_2 are spherically shape with diameters ranged from 30 to 40 nm while the commercial are also spherically shape but with large diameters ranged from 124 to 206 nm.

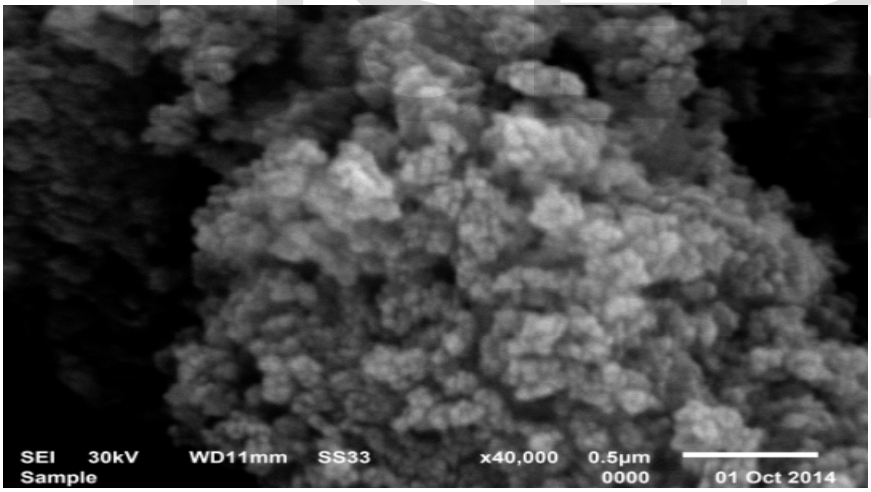

Fig. (7):SEM image of the synthesized ZnO (s).

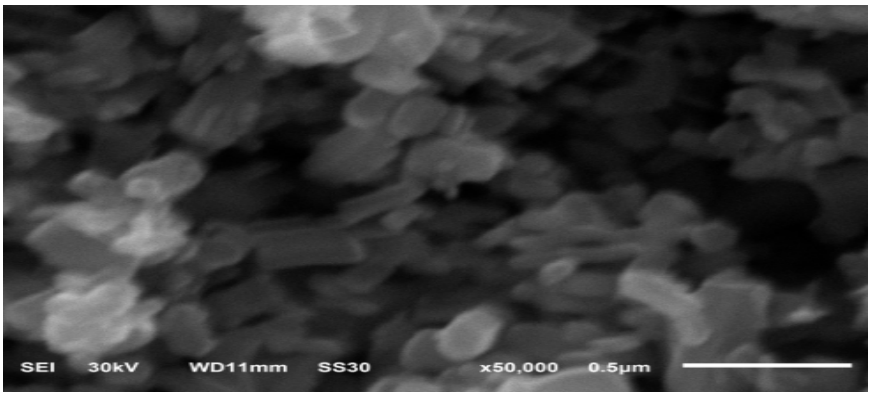

Fig. (8): SEM image of commercial ZnO.

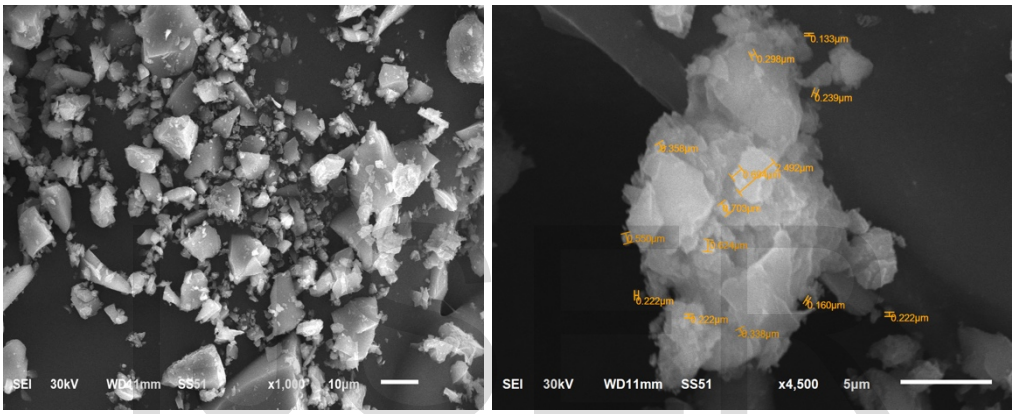

Fig. (9): SEM images of the synthesized TiO_2 (s).

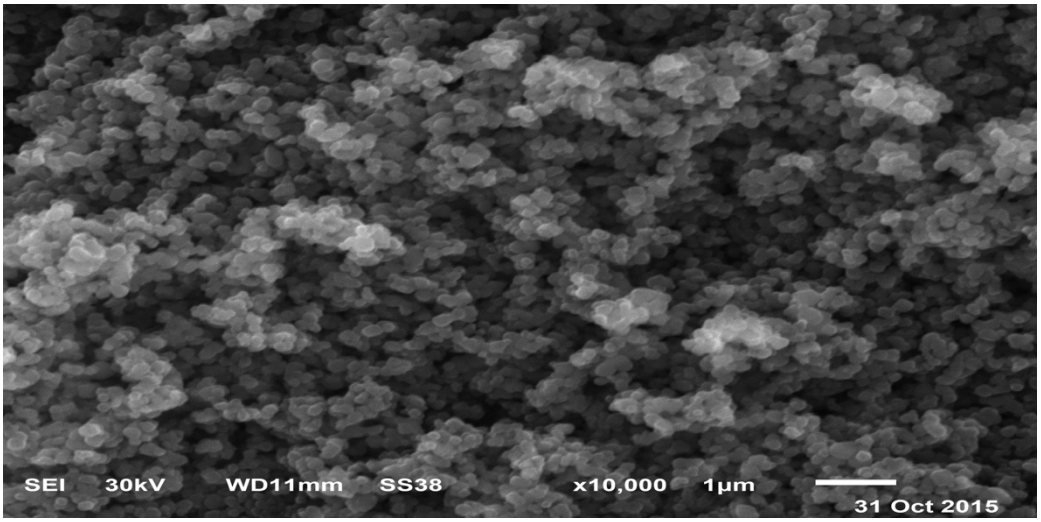

Fig. (10): SEM images of the commercial TiO_2.

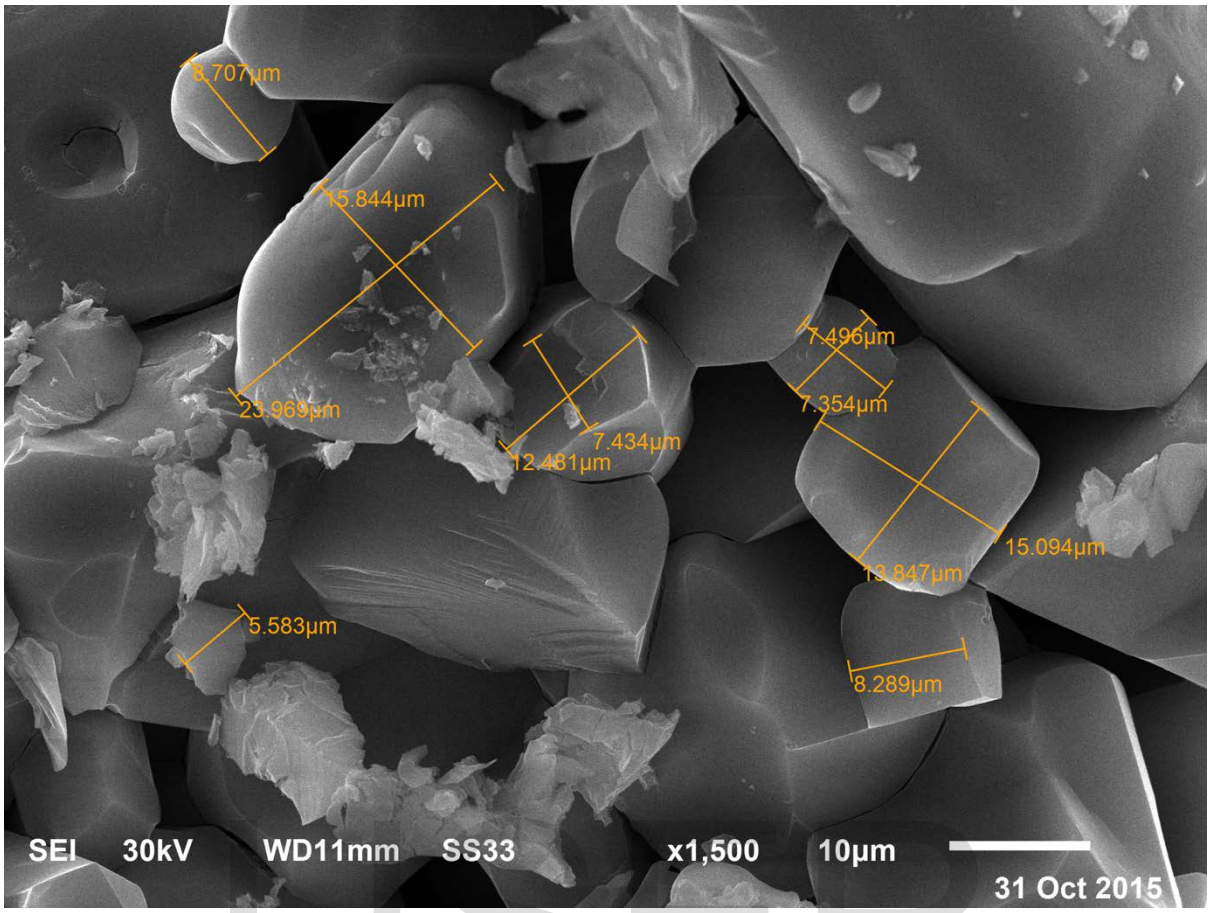

Fig. (11): SEM images of the commercial Fe.

3.1.6.Transmission Electron Microscope (TEM)

Additional studies on the structures of ZnO synthesized and commercial and as well as TiO_2 synthesized and commercial were done using transmission electron microscopy. Figure (12) shows the transmission electron microscopy (TEM) image of the synthesized ZnO (s). This image shows that the shape of the most of these particles is spherical with small amount of hexagonal diameters. The diameter of the synthesized ZnO (s) lies in the 12.48-26.12 nm.

Figure (13) reflects the shape of the commercial ZnO which appears as nanorods (nanowire) with hexagonal diameters lies in the range 30-83.87 nm and with length 70.96 -406.45 nm.

Figure (14) shows the transmission electron microscopy (TEM) image of the synthesized TiO_2. This image shows that the shape of the most of these particles is spherical with small amount of hexagonal diameters. The particle size was ranged from 8.52 to 34.56 nm.

Figure (15) reflects the shape of the commercial TiO_2 which appears as is spherical with small amount of hexagonal diameters lies in the range 33.33-100 nm and with length 100-273.33nm. This image shows that the size of commercial TiO_2 is very consistent.

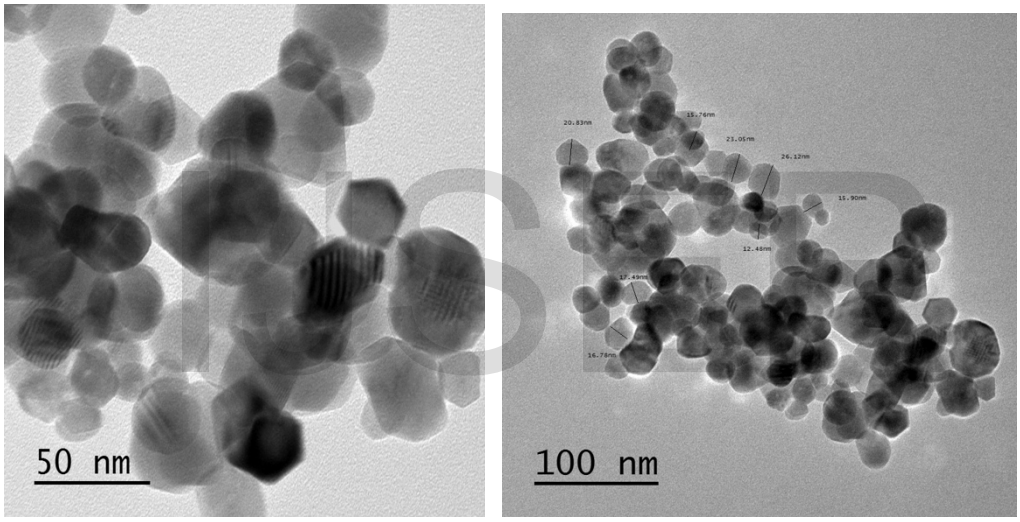

Fig. (12): TEM images of ZnO (NPs).

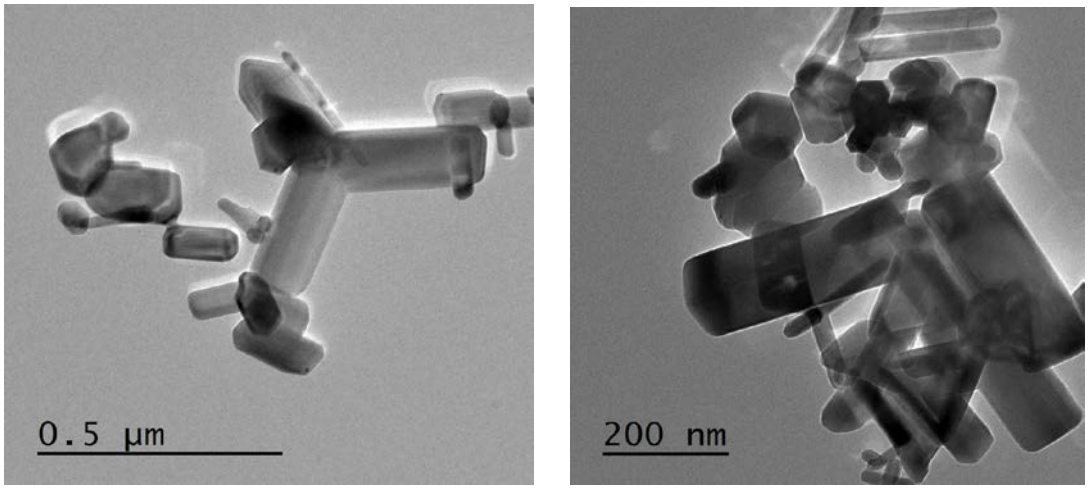

Fig. (13): TEM images of ZnO (c) nanorods.

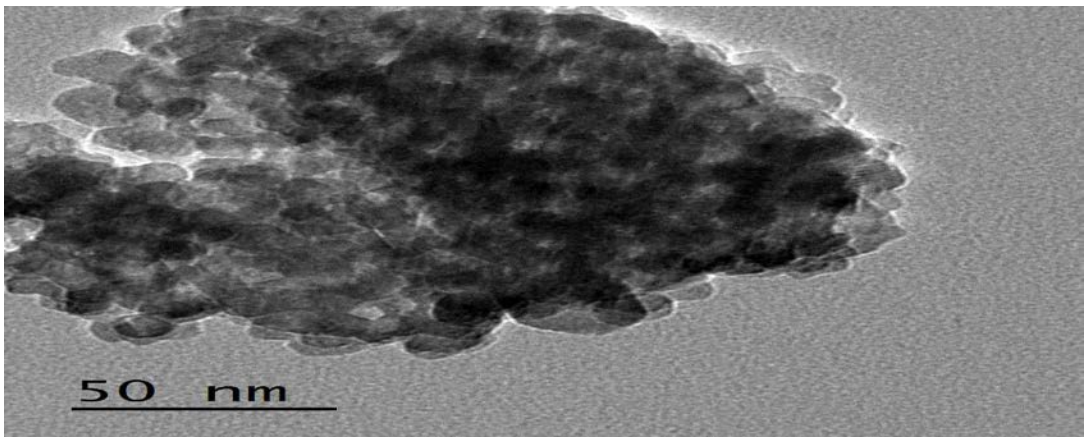

Fig. (14):TEM images of synthesized TiO_2 .

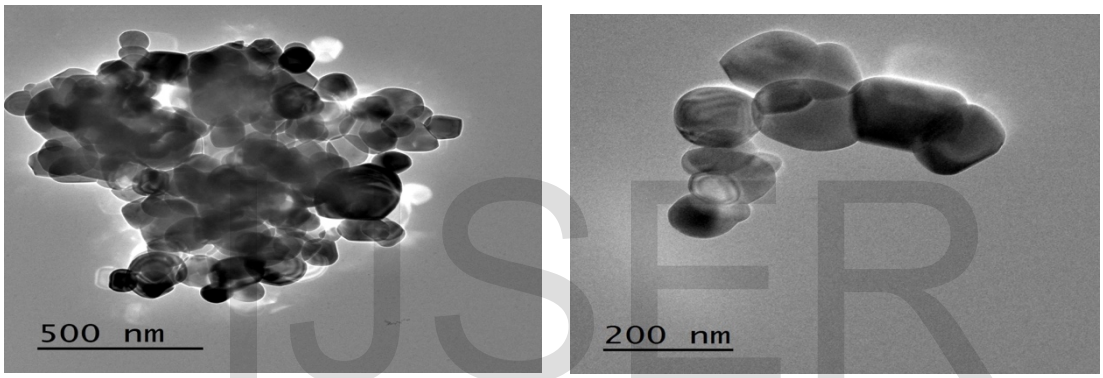

Fig. (15): TEM images of commercial TiO_2 (antase).

3.2.Degradation of lindane by advanced oxidation processes .

The first parameter considered in this study was the losses in lindane concentration with the irradiation time with respect to the rate and the complete degradation of the tested compound. As shown in Figure.16 as well, the irradiation under TiO_2(nano)/H_2O_2/UV, ZnO(nano)/H_2O_2/UV gave the highest degradation rate of lindane followed by Fe^{2+}/H_2O_2/UV, Fe^{3+}/H_2O_2/UV, TiO_2/H_2O_2/UV, ZnO/H_2O_2/UV, H_2O_2/UV and UV light alone, respectively. A complete degradation of lindane (100%) was achieved under TiO_2(nano)//H_2O_2/UV followed by ZnO(nano)/H_2O_2/UV, Fe^{2+}/H_2O_2/UV

$Fe^{3+}/H_2O_2/UV$, $TiO_2/H_2O_2/UV$, and $ZnO/H_2O_2/UV$ respectively systems within 0,10, 20, 40, 60, 80, 160, 320 and 360 min. of irradiation time, respectively (Figure 16). The complete degradation of the tested insecticide was not achieved under H_2O_2/UV and UV treatment.

Table (5) Degradation of lindane at initial concentration of 5ppm under UV, H_2O_2/UV, $Fe^{3+}/H_2O_2/UV$, $Fe^{2+}/H_2O_2/UV$, $ZnO(nano)/H_2O_2/UV$, $ZnO/H_2O_2/UV$, $TiO_2(nano)/H_2O_2/UV$ and $TiO_2/H_2O_2/UV$ systems by HPLC analysis.

Time (min)	UV	H_2O_2/ UV	$FeCl_3$/ H_2O_2/ Uv	$FeSO_4$/ H_2O_2/ UV	ZnO/ H_2O_2/ UV	ZnO(nano) H_2O_2/ UV	TiO_2/ H_2O_2/ UV	TiO_2(nano)/ H_2O_2/ UV
0	5	5	5	5	5	5	5	5
10	4.89	4.95	4.9	4.96	4.94	4.5	4.95	4.5
20	4.75	4.7	4.49	4.62	4.5	3	4.69	3.1
40	4.67	4.0	3.6	3.87	3.7	2.51	3.72	2.52
60	4.53	3.67	201	2.4	2.3	1.2	2.37	1.25
80	4.4	3.49	1.35	1.41	1.46	0.4	1.47	O.45
160	4.0	3.09	0.87	0.955	0.91	0.1	0.9	0.2
320	3.9	2.87	0.3	0.5	0.4	0.025	0.42	0.03
360	3.5	2.67	0.01	0.02	0.025	0.0	0.025	0

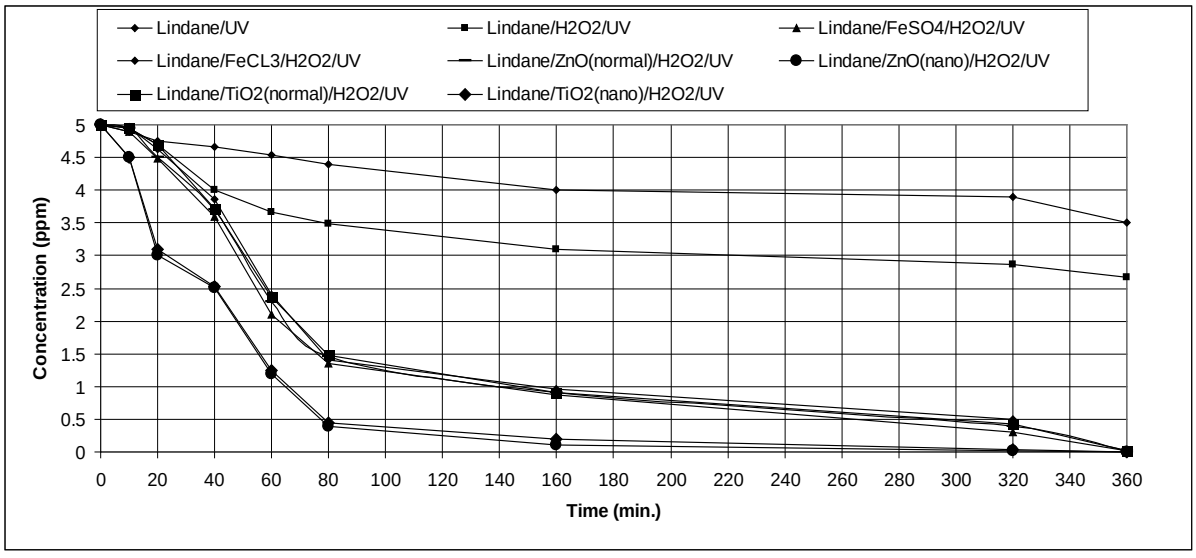

Fig. (16): Degradation of lindane at initial concentration of 5ppm under UV, H_2O_2/UV, $Fe^{3+}/H_2O_2/UV$, $Fe^{2+}/H_2O_2/UV$, $ZnO(nano)/H_2O_2/UV$, $ZnO/H_2O_2/UV$, $TiO_2(nano)/H_2O_2/UV$ and $TiO_2/H_2O_2/UV$ systems by HPLC analysis.

Table (6) Degradation of lindane at initial concentration of 5ppm under insecticide only, H_2O_2, Fe^{3+}/H_2O_2, Fe^{2+}/H_2O_2, ZnO(nano)/H_2O_2, ZnO/H_2O_2, TiO_2/H_2O_2 and TiO_2(nano)/H_2O_2 systems in dark conditions by HPLC analysis.

Time	Lindane	$FeCl_3/H_2O_2$	$FeCL_4/H_2O_2$	$FeSO_4/H_2O_2$	ZnO/H_2O_2	ZnO(nano) / H_2O_2	TiO_2/H_2O_2	TiO_2(nano)/ H_2O_2
0	5	5	5	5	5	5	5	5
10	4.996	4.998	4.998	4.999	4.995	4.99	4.999	4.998
20	4.992	4.996	4.989	4.998	4.989	4.988	4.998	4.992
40	4.988	4.992	4.972	4.985	4.985	4.987	4.985	4.986
60	4.985	4.989	4.968	4.979	4.977	4.986	4,979	4,98
80	4.981	4.985	4.961	4.975	4.969	4.982	4.975	4.974
160	4.977	4.97	4.957	4.968	4.967	4.961	4.968	4.961
320	4.973	4.965	4.95	4.959	4.966	4.94	4.967	4.945
360	4.970	4.96	4.948	4.95	4.96	4.923	4.961	4.928

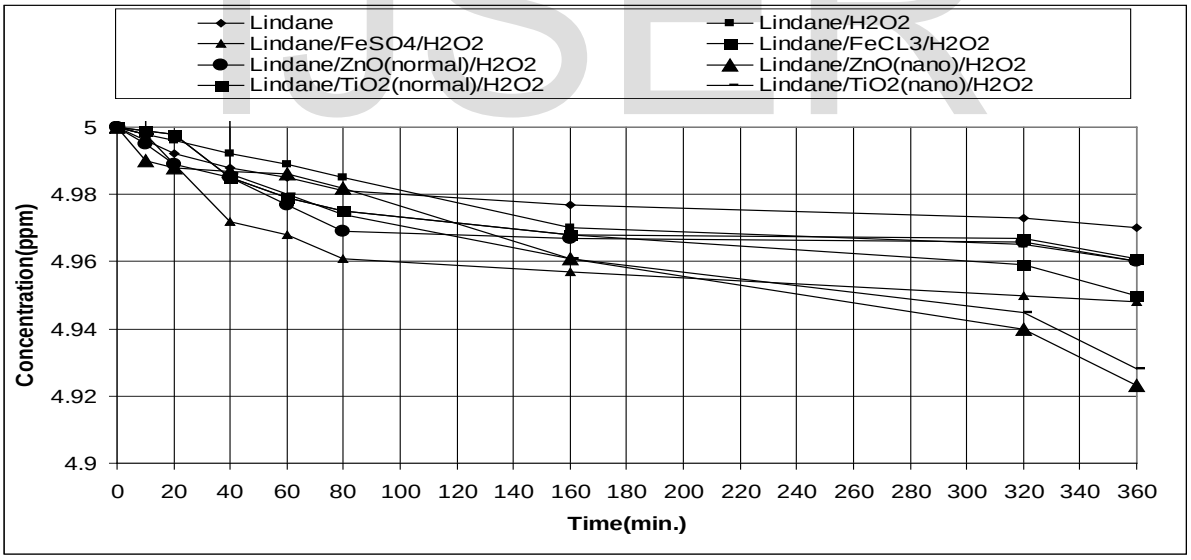

Fig.(17): Degradation of lindane at initial concentration of 5ppm under insecticide only, H_2O_2, Fe^{3+}/H_2O_2, Fe^{2+}/H_2O_2, ZnO(nano)/H_2O_2, ZnO/H_2O_2, TiO_2/H_2O_2 and TiO_2(nano)/H_2O_2 systems in dark conditions by HPLC analysis.

The degradation of the tested insecticide (lindane) under dark condition was very slow compared with the degradation rate under light conditions. As

shown in Figure (17) as well, the irradiation under TiO_2(nano)//H_2O_2, ZnO(nano)/H_2O_2 gave the highest degradation rate of lindane followed by Fe^{2+}/H_2O_2, Fe^{3+}/H_2O_2, TiO_2/H_2O_2, ZnO/H_2O_2, H_2O_2/UV and pesticide alone, respectively within 0, 10, 20, 40, 60,80,160, 320 and 360 min of time. The degradation rate of lindane treatments ranged from 0.6 to 1.54%.

The results showed that, the degradation rate of lindane was enhanced by irradiation under TiO_2(nano)//H_2O_2/UV and ZnO (nano)/H_2O_2/UV relative to the degradation under other photochemical remediation systems. This enhancement in lindane degradation rate under TiO_2(nano)//H_2O_2/UV and ZnO(nano)/H_2O_2/UV compared to other photochemical irradiation systems is due to the facts that the stabilized nanoparticles offer much greater surface area and reactivity which lead to higher generation rate of hydroxyl radicals relative to the normal particles (**He and Zhao, 2005; He et al. 2007**).

After 80 min of irradiation time, the degradation rate of the remaining lindane was quite slower than the first 80 min under all photochemical remediation systems. This is might be due to the low concentration of the remaining lindane (lower than 20% of initial concentration) after 80 min of irradiation time which lead to high delivery rate of Fe^{3+}/H_2O_2/UV, TiO_2/H_2O_2/UV, ZnO/H_2O_2/UV and H_2O_2/UV corresponds to higher concentrations of these reagents, and this subsequently increase their ability to compete with lindane to react with hydroxyl radicals as hydroxyl radicals scavenger (esq. 1,2) **[Catastini et al. 2002; El-Morsi et al. 2002: Wang and Lemely, 2002 and Derbalah, 2009].** Also, chloride and carbonate ions naturally

present in water react as hydroxyl radical scavenger (**Pare et al. 2008**) as shown in equations 3 and 4.

$$Fe^{2+} + {}^{\cdot}OH \rightarrow Fe^{3+} + + OH \quad (1)$$

$${}^{\cdot}OH + H_2O_2 \rightarrow HO_2^{\cdot} + H2O \quad (2)$$

$$Cl^{-} + {}^{\cdot}OH \rightarrow Cl^{\cdot} + + OH^{-} \quad (3)$$

$$CO_3^{-2} + {}^{\cdot}OH \rightarrow CO_3^{-\cdot} + OH^{-} \quad (4)$$

The degradation rate of lindane under $Fe^{2+}/H_2O_2/UV$ was higher than that under $ZnO/H_2O_2/UV$. This is may be due to the high generation rate of hydroxyl radicals under $Fe^{2+}/H_2O_2/UV$ (nano or normal) through many resources (Eqs. 5-8) relative to $ZnO/H_2O_2/UV$ (nano or normal) (eqs. 7-10) (**Derbalah, 2009**).

$$H_2O_2 + h\nu \rightarrow 2\ {}^{\cdot}OH \quad (5)$$

$$Fe^{3+} + H_2O_2 \rightarrow Fe^{2+} + HO_2^{\cdot} + H \quad (6)$$

$$Fe^{2+} + H_2O_2 \rightarrow Fe^{3+} + {}^{\cdot}OH + OH^{-} \quad (7)$$

$$Fe(OH)^{2+} + h\nu \rightarrow Fe^{2+} + {}^{\cdot}OH \quad (8)$$

$$ZnO + h\upsilon \rightarrow ZnO\ (e_{-\,cb} / h_{+\,vb}) \rightarrow e_{-cb} + h_{+\,vb} \quad (9)$$

$$e_{-\,cb} + h_{+\,vb} \rightarrow \text{heat} \quad (10)$$

$$h_{+\,vb} + OH- \text{ (or } H_2O)ads \rightarrow \bullet OH\ (+ H+) \quad (11)$$

$$e_{-\,cb} + O_2 \rightarrow \bullet O_2^{-} \quad (12)$$

$TiO_2/H_2O_2/UV$ showed high ability for the degradation of the tested insecticides (**Kouloumbos *et al.*, 2003**). This high degradation due to that the semiconductor TiO_2 in the presence of light, valence band holes (h^{+}_{vb}) and conduction band electrons (e^{-}_{cb}) are photogenerated (eq. 12). OH radicals

generated through water oxidation by photo-generated valence band holes according to eqs.13,14 and 15 are known to be the most oxidizing species. OH radicals react rapidly and non-selectively with organic molecules leading to the production of numerous oxidation intermediates and final mineralization products. In the presence of air, other species might contribute to the oxidation of the organic molecules, such as H_2O_2 or even superoxide radicals, which are produced by oxygen reduction through photogenerated conduction band electrons.

$$TiO_2 + h\upsilon \rightarrow e_{-cb} + h_{+\,vb} \quad (13)$$

$$TiO_2\,(h+) + H_2O_{ad} \rightarrow TiO_2 + \bullet OH + H \quad (14)$$

$$TiO_2\,(h+) + HO_{ad} \rightarrow TiO_2 + \bullet OH \quad (15)$$

$$TiO_2\,(h+) + RX_{ad} \rightarrow TiO_2 + RX^{\cdot +} \quad (16)$$

The degradation rate of lindane under ZnO (nano)/H_2O_2/UV was higher than that under ZnO/H_2O_2/UV and this due to the effect of particle size of nano zinc oxide. The effect of particle size on the photodegradation efficiency can be ascribed to two reasons. (1) When the size of ZnO crystals decreases, the amount of the dispersion particles per volume in the solution will increase, resulting in the enhancement of the photon absorbance. (2) The surface area of ZnO photocatalyst will increase as the size of ZnO crystals decreases, which will promote the adsorption of more insecticide molecules on the surface [**Wang et al. 2007**].

The degradation rate of lindane under TiO_2(nano)//H_2O_2/UV was higher than that under TiO_2/H_2O_2/UV and this due to the effect of nano ferric oxide particle size which agree with **Valdés-Solís et al. (2007a, b)** who developed a new catalyst using

nanosize particles with a high surface area that can accelerate the Fenton-like reaction without requiring UV radiation.

The titanium and zinc oxide nanocatalysts are very reactive because the active sites are located on the surface. As such, they have a low diffusional resistance, and are easily accessible, to the substrate molecules. Nanocatalysis is but one of the many practical applications of nanotechnology which is concerned with the synthesis and functions of materials at the nanoscale range (b100 nm) (**Mamalis, 2007; Miyazaki and Islam, 2007; Lines, 2008**). An important feature of nanomaterials is that their surface properties can be very different from those shown by their macroscopic or bulk counterparts (**Theng and Yuan, 2008**). As the term suggests, 'nanocatalysis' uses nanoparticles and nanosize porous supports with controlled shapes and sizes (**Bell 2003**). The application of nanoparticles as catalysts of the Fenton-like and photo-Fenton reactions has been described by several investigators (**Feng et al. 2004a, b; Valdés-Solís et al. 2007a, b; Zelmanov and Semiat, 2008)**. In comparison with their microsize counterparts, nanoparticles show a higher catalytic activity because of their large specific surface where catalytically active sites are exposed (**Nurmi et al. 2005**). Form all previous discussion titanium dioxide and zinc oxide nanoparticles are potentially useful for remediation of lindane in water because they can reach or penetrate into zones that are inaccessible to microsize solid catalysts **Liu (2006)**. Lindane (γ-HCH) is the most polar and most reactive isomer of all HCH isomers. The known a biotic degradation pathways of the HCHs include base-catalyzed dehydrohalogenation and metal-mediated dihalo-elimination (or b-elimination) (**Joo and Zhao, 2008**).

Table (7) Photochemical degradation of lindane at initial concentration 5 ppm under ZnO(c)/H_2O_2/sunlight, ZnO(s)/H_2O_2/sunlight and sunlight alone systems using HPLC analysis.

Time (min)	Lindane + sun	Lindane+ZnO (normal)+ H_2O_2 + sun	Lindane +ZnO (nano)+ H_2O_2 +sun
0	5	5	5
10	5	4.98	4.9
20	4.89	4.39	4.25
40	4.76	3,8	3.75
60	4.69	3.2	2.54
80	4.495	2.6	1.75
160	4.368	1.4	1.25
320	4.24	0.8	0.6
360	4	0.5	0.012

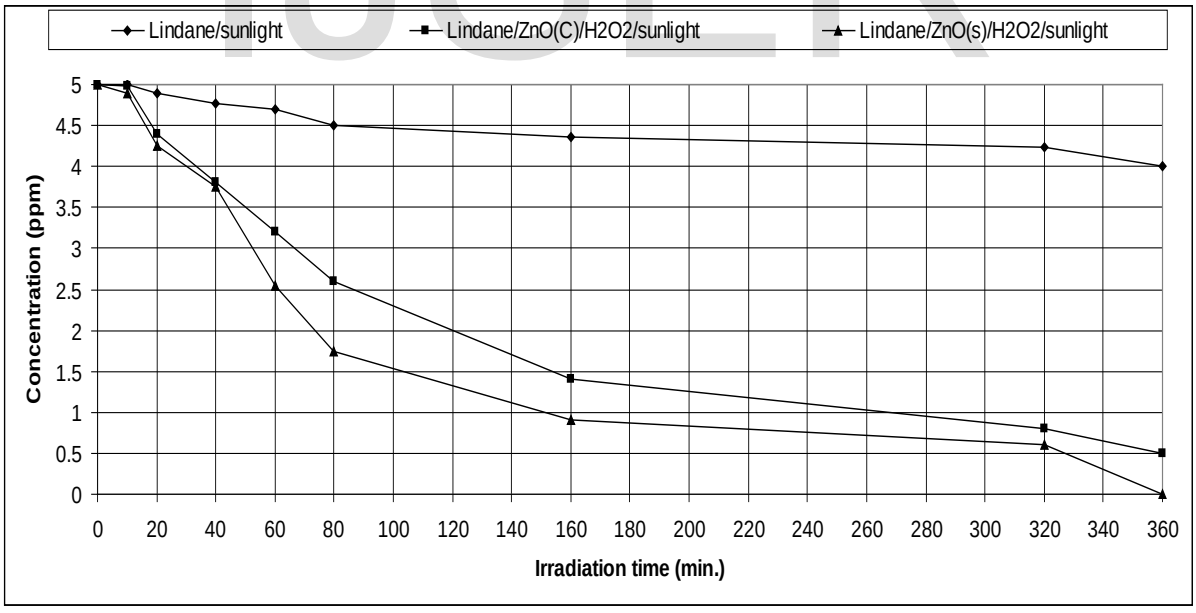

Fig (18) Photochemical degradation of lindane at initial concentration 5 ppm under ZnO(c)/H_2O_2/sunlight, ZnO(s)/H_2O_2/sunlight and sunlight alone systems using HPLC analysis.

From previous results it could be summarized that, the photocatalytic degradation of pesticides in general, and chlorinated hydrocarbons in particularly. Lindane as long life resistance in soil and in water have a good stability chemical structure and resist against degradation. Therefore the use of advanced oxidation processes in presence of ZnO or TiO_2 in nanoparticles play an important role for the mechanism of the chemical degradation. The nanoparticles exhibit photocatalytic activity and the mechanism might be due to cascade electron transfer in the ternary phase, more over the semiconductors photocatalysis process utilizes energy from UV light and solar light and the process can be described as:-

$$\text{Organic pollutants} + O \xrightarrow[\text{Semiconductor}]{h\nu \geq Eg} CO_2 + H_2O + \text{minerals}$$

Minerals are generated from hetero atoms such as S, N and Cl containing organo pollutants such as Lindane and Eg is the bandgap of the semiconductor and during the photocatalytic process, electron hole pairs are generated in valence and conduction bands of a semiconductor due to presence of fee radical, attack the molecules of pollutants. (Dhal, et. al., 2015). Masoud, 1988 reported that, the foliar fertilizer may influence to outcome of photochemical reaction in two different ways: (1) they can be photosensitizer or (2) they can act as the reaction partner to the pesticide molecule energized by light.

3.3.Biodegradation of Lindane using microbe isolates

The degradation ability of the *Xanthomonas campestris pv. Translucens* and *Aspergillus fumigatus* isolates against lindane was illustrated in Figure (19). *Xanthomonas campestris pv. Translucens* and *Aspergillus fumigatus* showed high

potential in the degradation of the tested insecticide**.** 94% of lindane initial concentration (5 mg L^{-1}) was degraded within 32 days by *Xanthomonas campestris pv. Translucens* while 84% of lindane was degraded within the same time by *Aspergillus fumigatus.*

Table (8) Biodegradation of lindane at concentration level 5ppm by *Xanthomonas campestris pv. Translucens* and *Aspergillus fumigatus* in aqueous media.

Time	Lindane +Xanthomonas Campestris pv. Translucens	Lindane+ Aspergillus fumigatus	Lindane+ MSL (Control)
0	**5**	**5**	**5**
10	**4.89**	**4.98**	**4.99**
20	**3.82**	**3.93**	**4.985**
40	**3.23**	**3.4**	**4.981**
60	**2.65**	**2.9**	**4.971**
80	**2.06**	**2.31**	**4.963**
160	**1.47**	**1.76**	**4.958**
320	**0.88**	**231**	**4.953**
360	**0.30**	**0.80**	**4.94**

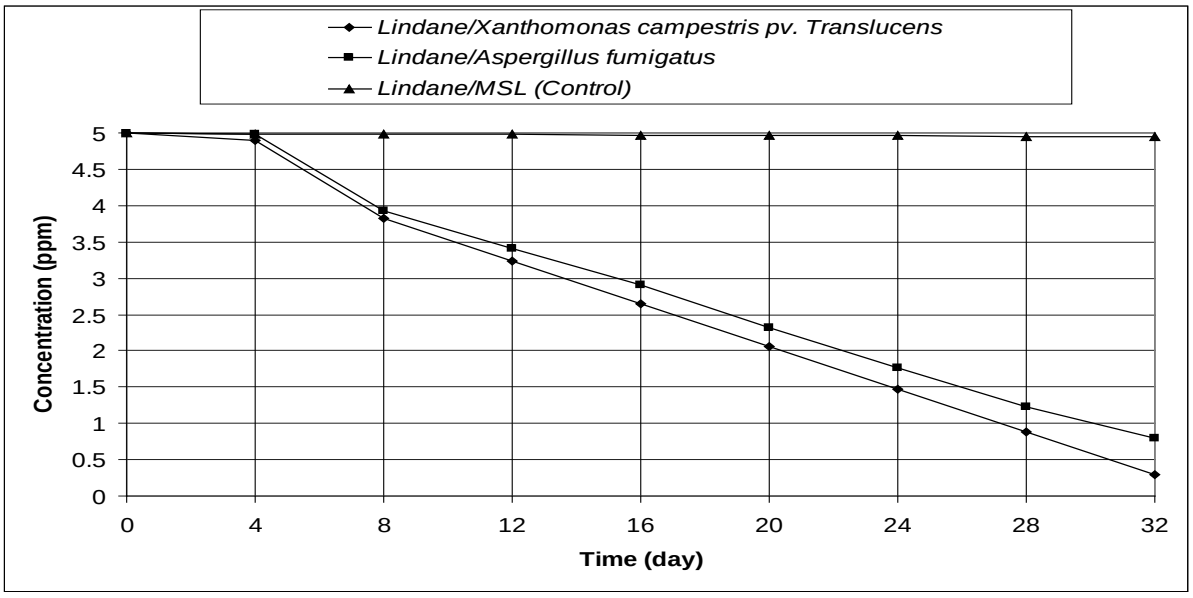

Fig. (19): Biodegradation of lindane at concentration level 5ppm by *Xanthomonas campestris pv. Translucens* and *Aspergillus fumigatus* in aqueous media.

On contrary, the degradation percentage of lindane reached to 1.2% at the end of incubation time in control or non-inoculated samples, was negligible at the end of incubation time in control samples. This is indicating that a biotic losses of lindane is negligible. This is implied that the quote of tested insecticide decay due to temperature effect and photodecomposition and volatilization is very slight or completely absent.

The degradation of the tested insecticide may be attributed to the secretion of enzymes from either tested bacterial or fungal strains which are capable of degrading pesticides (**Bollag and Liu, 1990**). On the other hand, the tested insecticide degradation percentage reached to 1.2% at the end of incubation time in control or non-inoculated samples. This is implied that the quote of tested insecticide decay due

to temperature effect, photodecomposition and volatilization is very slight or negligible.

Moreover, *Aspergillus fumigatus* showed a high efficiency of the tested insecticide degradation, which agrees with previous studies that reported that fungi showed a high potential for pesticide degradation **(Derbalah et al., 2008; Massoud et al., 2008)**. Isolates of *Xanthomonas campestris pv. Translucens* and *Aspergillus fumigatus* achieved highly efficient degradation of the tested insecticide. This study may be considered the first report on tested insecticide bioremediation and a key step in further studies on the tested insecticides microbial detoxification. Moreover, the tested microorganisms isolated from water could prove valuable in pesticide bioremediation in water system.

3.4. Toxicity assessment

3.4.1. The histopathological changes in the kidney

The normal structure of kidney tissue is shown in Figure 19A. For the rats treated with lindane after remediation with ZnO (nano)/H_2O_2/UV (B) and *Xanthomonas campestris pv. Translucens*(C) the tissues was normal as control (Fig.19 B-C)

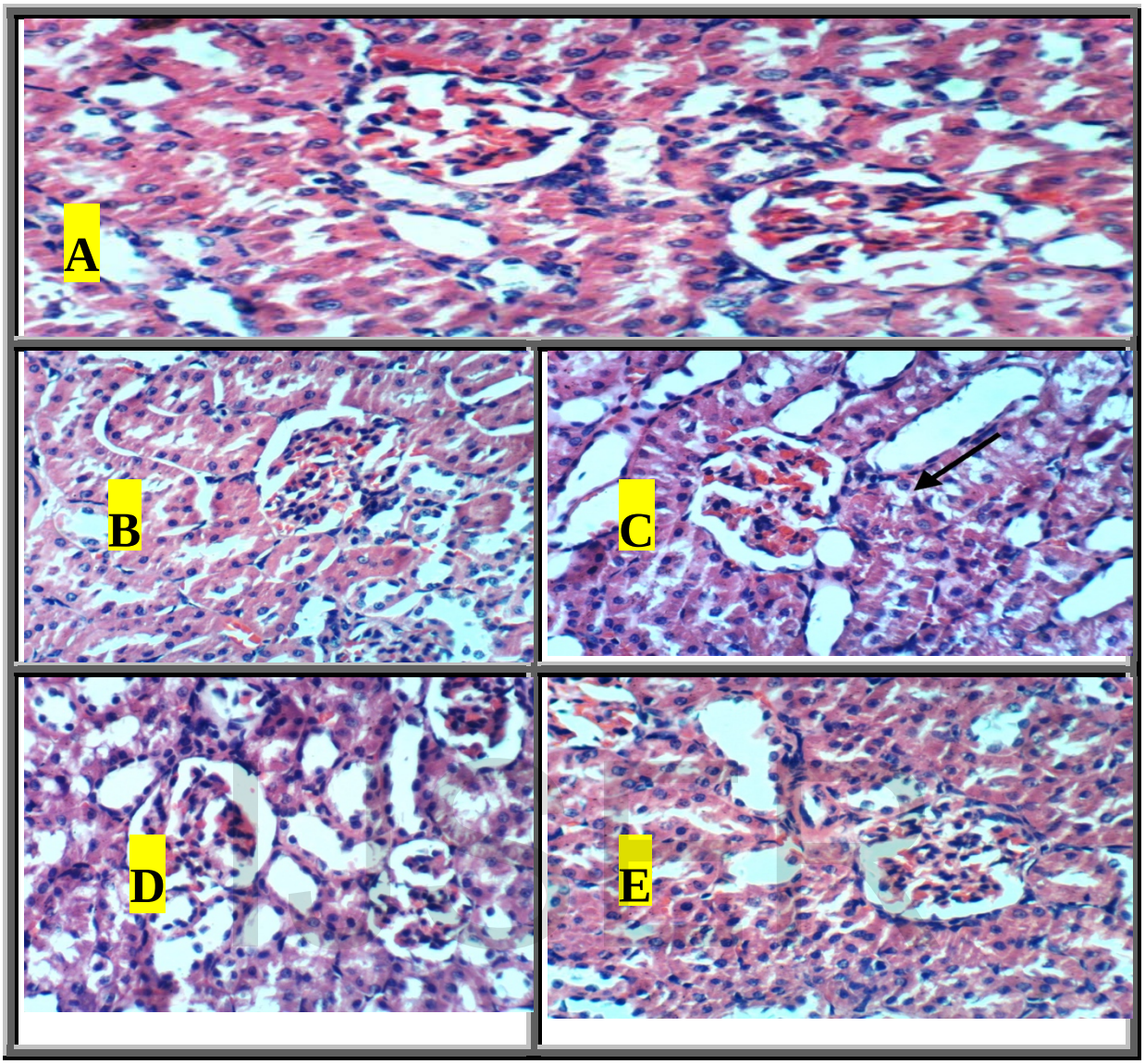

Fig. (19): Sections in kidney of rats treated with lindane-contianing water after remediation with ZnO (nano)/H_2O_2/UV (B), and *Xanthomonas campestris pv. Translucens*(C), as well as ZnO (nano)/H_2O_2 (D) and *Xanthomonas campestris pv. Translucens* (E) without lindane relative to control (A).

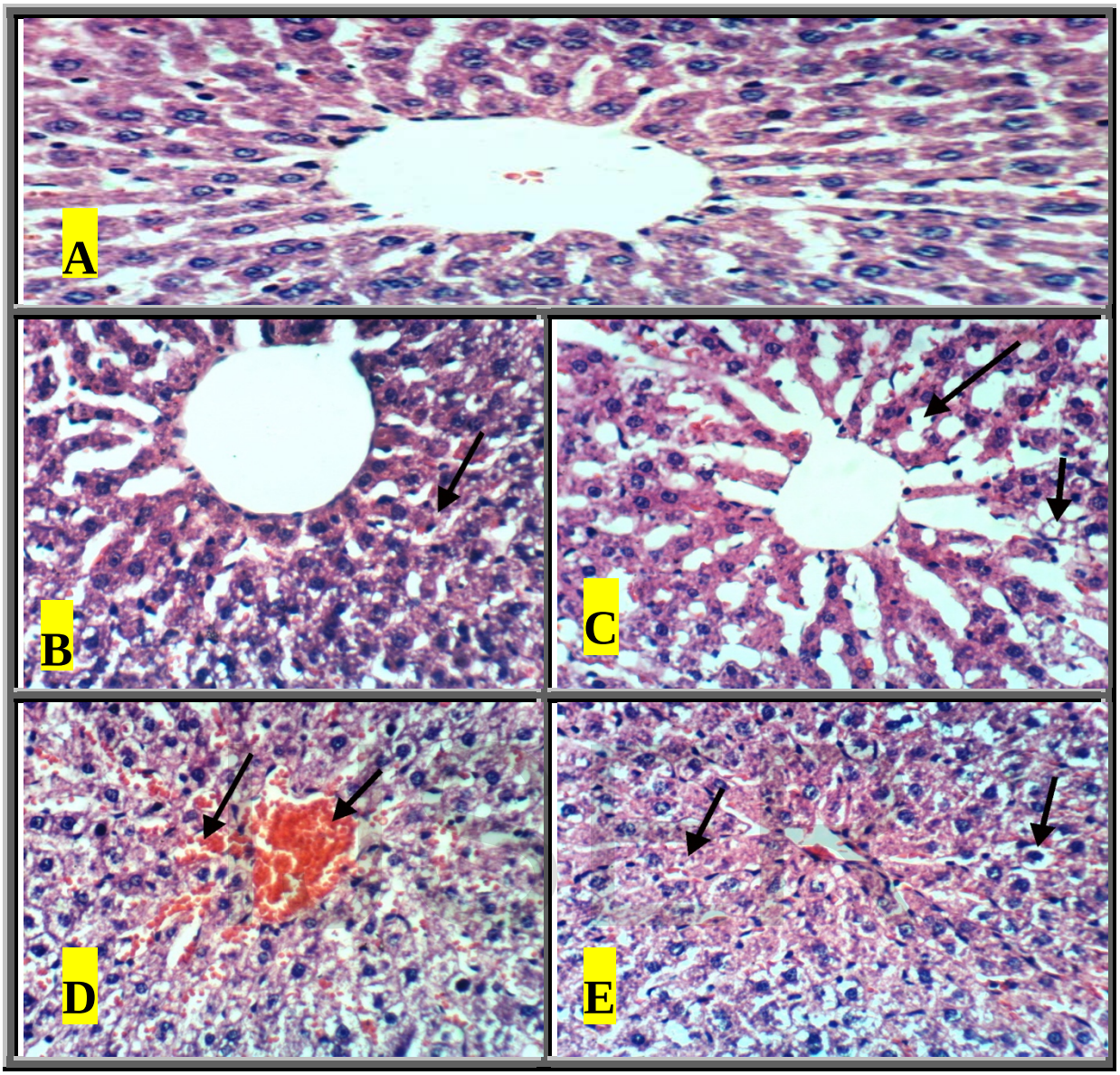

Fig. (20): Sections in liver of rats treated with lindane containing water after remediation with ZnO (nano)/H_2O_2/UV (B), and *Xanthomonas campestris pv. Translucens*(C), as well as ZnO (nano)/H_2O_2/UV and *Xanthomonas campestris pv. Translucens* (E) without lindane relative to control (A).

To confirm the safety of the most effective treatments that used in the remediation, some rats were treated with ZnO (nano)/H_2O_2/UV (D), and *Xanthomonas campestris pv. Translucens*(E), without lindane and the kidney tissues were normal as control.

3.4.2.The histopathological changes in the liver

The normal structure of liver tissue is shown in Fig. (20A). For the rats treated with lindane after remediation with ZnO (nano)/H_2O_2/UV (Fig.20 B), the tissue was normal like control with a mild changes such as dilatation of hepatic sinusoids. For the rats treated with lindane after remediation with *Xanthomonas campestris pv. Translucens*(C), the tissue was normal as control (Fig.20 C) with a moderate changes like cytoplasmic vacuolization of hepatocytes and dilatation of hepatic sinusoids. To confirm the safety of materials used in the remediation, some rats were treated with ZnO (nano)/H_2O_2/UV (D), and *Xanthomonas campestris pv. Translucens*(E), without lindane and the kidney tissues were normal as control with a mild changes such as congestion of central vein (Fig. 19 D) and slight hydropic degeneration of hepatocytes (Fig. 19 E) .

To evaluate the efficacy of different tested remediation techniques in removing lindane from drinking water, toxicity assessment was carried out with respect to histology test. The histological test for all remediation techniques of lindane in water showed no significant changes in kidney or liver of treated rats relative to control treatment. This implies that lindane which spiked water samples before remediation was completely removed in all remediation techniques. Also, this is implying the safety of all tested chemical and biological remediation techniques on

human health especially when we extend the remediation time for photochemical and bioremediation techniques

4.Conclusions

The photo titanium dioxide and photo zinc oxide combined with hydrogen peroxide showed much promise in the complete degradation and detoxification of lindane in contaminated water, especially by using titanium and zinc oxide nanoparticles. *Xanthomonas campestris pv. Translucens* and *Aspergillus fumigatus* are promising as effective and safe bioremediation for lindane removal in water.

5.References

Abou-Arab, A. A. K.; Gomaa, M. N. E.; Badawy, A.; Naguib, K. (1995) Distribution of organochlorine pesticides in the Egyptian aquatic ecosystem. *Food Chemi.*, 54:141-146.

Addamo, M.;V. Augugliaro.; A. DiPaola.; E. Garcıa-Lo pez.; V. Loddo.; G. Marcı.; R. Molinari.; L. Palmisano.; M. Schiavello. (2004). J. Phys. Chem. B108: 3303-3310 pp.

Bancroft, J. D.; Stevens, A. (1996) Theory and Practice of Histological Techniques. Fourth edition. Churchill-Livingstone London.

Bell, A.T. (2003). The impact of nanoscience on heterogeneous catalysis. *Sci.* 299, 1688–1691.

Benitez, F. J.; Acero, J. L.; Real, F.J. (2002) Degradation of carbofuran by using ozone, UV radiation and advanced oxidation processes. *J. of Hazard Mat*. 89, 51-65.

Bollag, J. M.; Liu. S. Y. (1990). Biological transformation process of pesticides. Pesticides in the Soil Environment (ed. Chang H.H.) Soil Science Society of America, Madison, WI. 169-211.

Boonyatumanond, R.; Jaksakul, A.; Puncharoen, P.; Tabucanon, M. S. (2002) Monitoring of organochlorine pesticides residues in green mussels (*Perna viridis*) from the coastal area of Thailand. *Environ. Pollut*. 119, 245-252.

Caroline, A. H. Michael, W.W.; Alastair, W. M. H. (2001) Factors affecting the transfer of organochlorine pesticide residues to breast milk. *Chemosphere* 43, 243-256.

Catastini, C.; Sarakha, M.; Mailhot, G.; Bolte, M. (2002) Iron(III) aquacomplesxes as effective photocatalysis for the degradation of pesticides in homogenous aqueous solutions. *Sci. of Tot. Environ*. 298, 219-228.

Chang, S.; and Doong, R. (2006) Concentration and fate of persistent organochlorine pesticide in estuarine sediments using headspace solid-phase microextraction 2006. *Chemosphere*. **62**:1869-1878.

Derbalah, A. S. (2009) Chemical remediation of carbofuran insecticide in aquatic system by advanced oxidation processes. J. Agric. Res. Kafrelsheikh Univ. 35, 308-327.

Derbalah, A. S. Nakatani, N. ; Sakugawa, H. (2004) Photocatalytic removal of fenitrothion in pure and natural waters by photo-Fenton reaction. *Chemosphere*.57, 635-644.

Derbalah, A. S.; Massoud, A. H.; Belal, E. B. (2008) Biodegrability of famoxadone by various microbial isolates in aquatic system. *Land Contam. & Reclamat*. 16, 13-23.

Derbalah. A. S.; Belal, E. B. (2008). Biodegradation kinetics of cymoxanil in aquatic system. Chemistry and Ecology. 3: 169-180.

Dhal, J. P.; B. G. Mishra and G. Hota. (2015). Hydrothermal synthesis and enhanced photocatalytic activity of ternary $Fe_2O_3/ZnFe_2O_4$/ ZnO nanocomposite through cascade electron transfer. RSC Adv., 5: 58072.

El-Kemary, M.; H. El-Shamy and I. El-Mehasseb. (2010). Photocatalytic degradation of ciprofloxacin drug in water using ZnO nanoparticles. Journal of Luminescence. 130: 2327-2331pp.

El-Morsi, T. M.; Emara, M. M. Abd El Bary, H. M. H. Abd El-Aziz, A.; Friesen, K. J. (2002) Homogeneous degradation of 1,2<10 tetrachlorodecane in aqueous solutions using hydrogen peroxide, iron and UV light. *Chemosphere.* 47, 343-348.

Evgenidou, E.; K. Fytianos and I. Poulios (2005). Photocatalytic oxidation of dimethoate in aqueous solutions. Journal of Photochemistry and Photobiology A: Chemistry. 175: 29-38.

Feng, J.; Hu, X.; Yue, P. L. (2004a) Novel bentonite clay-based Fe-nanocomposite as a heterogeneous catalyst for photo-Fenton discoloration and mineralization of Orange II. *Environ. Sci. Technol*. 38, 269-275.

Feng, J.; Hu, X.; Yue, P. L. (2004b) Discoloration and mineralization of Orange II using different heterogeneous catalysts containing Fe: a comparative study. *Environ. Sci. Technol*. 38, 5773-5778.

Glynn, P. W.; Rumbold, D. G. and Snedaker S. C.(1995) Organochlorine pesticide residues in marine sediment and Biota from the Northern Florida Reef Tract. Marine Pollution Bulletin. 30 (6) pp.:397-402.

He, F.; Zhao, D. (2005) Preparation and characterization of a new class of starch-stabilized bimetallic nanoparticles for degradation of chlorinated hydrocarbons in water. *Environ. Sci. Technol*. 39, 3314-3320.

He, F.; Zhao, D. Liu, J.; Roberts, C.B. (2007) Stabilization of Fe–Pd nanoparticles with sodium carboxymethyl cellulose for enhanced transport and dechlorination of trichloroethylene in soil and groundwater. *Ind. Eng Chem Res* 46, 29-34.

Joo, S. H.; Zhao, D. (2008) Destruction of lindane and atrazine using stabilized iron nanoparticles under aerobic and anaerobic conditions: effects of catalyst and stabilizer. Chemosphere. 70:418-425.

Kouloumbos, V. N., Tsipi.; D. F., Hiskia, A.E., Nikolic, D. and Van Breemen, R.B.: Identification of photocatalytic degradation products of diazinon in TiO_2 aqueous suspensions using GC/MS/MS and LC/MS with quadrupole time-of-flight mass spectrometry. *J. Am. Mass Spectrom. 14*, 803-817 (2003).

Lines, M. G. (2008) Nanomaterials for practical functional uses. J. Alloys Compd. 449, 242-245.

Lino, C. M.; Silveira, M. I. N. (1997) Extraction and clean-up methods for the determination of organochlorine pesticide residues in medicinal plants. *J. Chromatogr. A* 769, 275-283.

Liu, W. T. (2006) Nanoparticles and their biological and environmental applications. *J Biosci. Bioeng*. 102, 1-7.

Mamalis, A.G. (2007) Recent advances in nanotechnology. *J Mater Process. Technol*. 181, 52-58.

Masoud, A.H; (1988) Photo degradation of some insecticides and their mixtures with foliar fertilizers. J. Agric.res. Tanta Univ., 14(2) (3), 1353-1360

Massoud A. H.; El-Fakhrany I. I.; Abd El-Razik, M. A. S. (2007a). Monitoring of some agrochemical pollutants in surface water in Kafr El-Sheikh Governorate. J. Pest. Cont. Environ. Sci., 15: 21-41.

Massoud, A. H.; Derbalah, A. S.; Belal E. B.; El-Fakhrany I. I. (2007b). Bioremediation of malathion in aquatic system by different microbial isolates. J. Pest Cont & Environ. Sci. 15(2):13-28.

Massoud, A. H.; Derbalah, A. S.; Belal, E. B. (2008). Microbial detoxification of metalaxyl in aquatic system. J. Environ. Sci., 20: 262-267.

Miyazaki, K. ; Islam, N. (2007) Nanotechnology systems of innovation an analysis of industry and academia research activities. *Technovation.* 27, 661-675.

Nurmi, J.; Tratnyek, P.G.; Sarathy, V.; Baer, D.R.; Amonette, J. E.; Pecher, K.; Wang, C.; Linehan, J.C.; Matson, D.W.; Penn R. L.; Driessen, M. D. (2005) Characterization and properties of metallic iron nanoparticle: spectroscopy, electrochemistry, and kinetics. *Environ. Sci. Technol*. 39, 1221–1230.

Pare, B. Singh, P. ; Jonnalagadda, S.B. (2008) Visible light induced heterogeneous advanced oxidation process to degrade pararosanilin dye in aqueous suspension of ZnO. *Indian J. of Chem*. 47, 830-835.

Pauwels, A.; Wells, D. A.; Covaci, A.; Schepens, P. J. C. (1999) Improved sample preparation method for selected persistent organochlorine pollutants in human serum using solid-phase disk extraction with gas chromatographic analysis. *J. Chromatogr B* 723, 117-125.

Rachel Carson (1962) Silent spring, Library of congress catalog card. Number : 60-5148.

Shannon, M. J.; Unterman, R. (1993) Evaluating bioremediation: distinguishing fact from fiction. *Annual Review of Microbiology* v47.(Annual 1993): pp715(24).

Theng, B. K. G.; Yuan, G. (2008) Nanopaticles in the soil environment. *Elements* 4, 395-399.

Tricklebank, K.A.; Kingsford, M. J.; Rose, H. A. (2002) Organochlorine pesticides and hexachlorobenzene along the central coast of New South Wales: multi-scale distributions using the territorial damsel fish *Parma microlepis* as an indicator. *Environ. Pollut.* 116, 319- 335.

Valdés-Solís, T. P.; Valle-Vigón, P.; Álvarez, S.; Marbán, G.; Fuertes, A. B. (2007b) Manganese ferrite nanoparticles synthesized through a nanocasting route as a highly active Fenton catalyst. *Catal. Commun.* 8, 2037-2042.

Valdés-Solís, T. P.; Valle-Vigón, P.; Sevilla, M.; Fuertes, A. B. (2007a) Encapsulation of nanosized catalysts in the hollow core of a mesoporous carbon capsule. *J. Catal.* 251, 239-243.

Wang, H. Xie, C. Zhang, W. Cai, S. Cai, Z. Yang, Z. ; Gui, Y. (2007) Comparison of dye degradation efficiency using ZnO powders with various size scales. *J. Hazard. Mat.* 141, 645-652.

Wang, Q.; Lemely, A.T. (2002) Oxidation of diazinon by anodic Fenton treatment. *Wat. Res.* 36, 3237-3244.

Vidali, M. (2001) Bioremediation. An overview. *Pure Appl. Chem.* 73, 1163-1172.

Zelmanov, G.; Semiat, R. (2008) Iron (3) oxide-based nanoparticles as catalysts in advanced organic aqueous oxidation. *Water Re*s. 42, 492-498.